

CNN Dynamics Represents a Broader Class than PDEs

M. Gilli*, T. Roska**, L. O. Chua⁺, and P. P. Civalleri*.

* Department of Electronics, Politecnico di Torino, Italy.

** Comp. Automation Inst., Hungarian Academy of Science and Patzmany University, Hungary.

⁺ Nonlinear Electronics Labs, University of California - Berkeley, USA.

Abstract

The relationship between Cellular Nonlinear Networks (CNNs) and Partial Differential Equations (PDEs) is investigated. The equivalence between discrete-space CNN models and continuous-space PDE models is rigorously defined. The key role of space discretization is explained. The problem of the equivalence is split into two sub-problems: approximation and topological equivalence, that can be explicitly studied for any CNN models. It is known that each PDE can be approximated by a space difference scheme, i.e. a CNN model, that presents a similar dynamic behavior. It is shown, through several examples, that there exist CNN models that are not equivalent to any PDEs, either because they do not approximate any PDE models, or because they have a qualitatively different dynamic behavior (i.e they are not topologically equivalent to the PDE, that approximate). This proves that the spatio-temporal CNN dynamics is broader than that described by PDEs.

1 Introduction

Cellular Neural/Nonlinear Networks (CNNs) are analog dynamic processors arrays [Chua & Yang, 1988a; Chua & Yang, 1988b; Chua & Roska, 1993a; Chua & Roska, 2002]. A CNN can be described as a 2 or n -dimensional array of identical nonlinear dynamical systems (called cells), that are locally interconnected. A stored programmable array computer combining CNN dynamics with logic (analogic array) has been invented [Chua & Roska, 1993b], keeping the mainly locally connected property. The latter property has allowed the realization of several high-speed VLSI chips [Vazquez *et al.*, 2000]. In most applications the connections are specified through space-invariant templates (that consist of small sets of parameters identical for all the cells) [Chua & Roska, 2002]. The mathematical model of a CNN consists of a large set of coupled nonlinear ordinary differential equations (ODEs), henceforth called canonical CNN equations, that may exhibit a rich spatio-temporal dynamics.

Partial Differential Equations (PDEs) are well known models for describing many classical spatio-temporal phenomena, occurring in physics, chemistry and biology [Whitham, 1968].

The relationship between canonical CNN equations and PDEs was investigated in several papers: in [Chua *et al.*, 1995] it was shown that CNNs are a paradigm for several spatio-temporal phenomena, occurring in reaction diffusion PDEs; in [Roska *et al.*, 1995; Kozek *et al.*, 1995] some basic methods for simulating linear and nonlinear PDEs, through CNNs, are introduced and some significant examples are given; in [Civalleri & Gilli, 1995] it is shown that CNN circuit models are suitable for simulating even nonlinear fluid dynamic equations, because they can preserve the physical properties of the continuous structure; in [Serpico *et al.*, 1999] the dynamic behavior of 1D CNNs is examined in detail, with reference to the properties of the corresponding continuous PDEs.

It is known that each PDE can be approximated by space difference schemes, that present a similar dynamic behavior: such schemes can be interpreted as suitable CNNs described by ODEs [Roska *et al.*,

1995; Godunov, 1987; Ames, 1977]. On the other hand it is shown in [Keener, 1987; Perez-Munuzuri *et al.*, 1993] that there are some spatio-temporal phenomena, like propagation failure, that can only be observed in spatially discrete structures and not in their continuous counterpart.

It is therefore important to investigate in a rigorous way the relationship between CNNs and PDEs, in order to determine which are the conditions under which the dynamic behavior of a CNN is similar (i.e. equivalent) to that of a given PDE. Such a study, that has not been carried out in the above mentioned papers [Chua *et al.*, 1995; Serpico *et al.*, 1999], is essential for establishing if we may expect that CNN dynamics is broader than PDE dynamics.

The paper is organized as follows. In Section 2 we present some characteristic and preliminary examples, that clarify the importance of studying the relationship between CNNs and PDEs. In Section 3 we identify the mathematical model of a substantial class of CNNs, that we call canonical CNN equations. We rigorously define the notion of equivalence between a canonical CNN equation and a PDE model. We show that the equivalence problem can be split into two sub-problems: approximation and topological equivalence. We develop a general technique, based on Taylor series expansion, for verifying that a canonical CNN equation approximates a PDE model; then we show that the study of the topological equivalence can be carried out through bifurcation analysis, by assuming as bifurcation parameters the space discretization steps. Finally in Section 4, through some significant examples, we show that there exist canonical CNN equations that are not equivalent to any PDEs, either because they do not approximate any PDE models, or because they are not topologically equivalent to the PDE that approximate. This proves that the CNN spatio-temporal dynamics is broader than PDE dynamics.

2 Characteristic Examples

In order to make the essence of the study clear, we show two characteristic examples, where a given CNN cannot be represented by any PDEs.

In the first example we consider a CNN with a one-dimensional opposite-sign template, described by the following equation:

$$\frac{dx_i}{dt} = pf[x_i(t)] + sf[x_{i+1}(t)] - sf[x_{i-1}(t)] \quad (1)$$

where $f(\cdot)$ is assumed to be a $C^\infty(R)$ nonlinear function.

In order to determine if such a model admits of a PDE description, as a continuous limit in space, we consider the similar case of a RC electrical transmission line, that is described by the following PDE (called RC transmission line equation):

$$\frac{\partial v(t, z)}{\partial t} = \frac{1}{RC} \frac{\partial^2 v(t, z)}{\partial z^2} \quad (2)$$

where z represents the space variable, $v(t, z)$ denotes the line voltage, \mathcal{R} and \mathcal{C} are the unit-length resistance and capacitance respectively.

The corresponding space discrete structure is represented by the chain of identical lumped RC cells shown in Fig. 2. It is easily verified that the following equation holds, for the i -th cell:

$$\frac{dv_i(t)}{dt} = \frac{1}{RC} [v_{i-1}(t) - 2v_i(t) + v_{i+1}(t)] \quad (3)$$

It is well known that the transmission line equation (2) can be obtained from (3) by assuming that each cell time constant $\tau = RC$ tends to zero. In particular if we denote with h the space discretization step, Eq. (2) is obtained by assuming that $h \rightarrow 0$, $R = \mathcal{R}h$ and $C = \mathcal{C}h$.

A similar procedure, called time-scaling, can also be applied to Eq. (1). It consists of the following two steps: a) the time constant of each cell is written as $\tau = \tilde{\tau}h^\alpha$, $\alpha > 0$; b) Eq. (1) is rewritten with respect to the time variable $t' = \tau t$:

$$\frac{dx_i}{dt'} = \frac{1}{\tilde{\tau}} \frac{pf[x_i] + sf[x_{i+1}] - sf[x_{i-1}]}{h^\alpha} \quad (4)$$

It is easily seen that if $p \neq 0$ the above Eq. (4) does not implement any acceptable difference scheme for $h \rightarrow 0$ and therefore it does not approximate any PDE (see Example 1 of Sec. 4, for a rigorous proof).

It is worth noting that the time-scaling approach outlined above implies that all the template elements present the same dependence on the space-discretization step h , i.e. $1/h^\alpha$ for some $\alpha > 0$. However the relationship between CNN equations and PDEs should be studied under more general conditions, i.e. by assuming that each template element may be an arbitrary function of the space-discretization steps. Such a general case will be studied in detail in the next Section.

In the second example, we consider the space-discretization of the Nagumo equation, with zero-flux boundary conditions

$$\frac{dx_i(t)}{dt} = \frac{D}{h^2} [x_{i+1}(t) - 2x_i(t) + x_{i-1}(t)] + f[x_i(t)] \quad (5)$$

where D is the diffusion coefficient, and $f(\cdot)$ is the function reported in Eq. (36) of Sec. 4.

We will show in the next Section that the above CNN equation, approximates for $h \rightarrow 0$ the continuous Nagumo equation (where z denote the continuous space variable)

$$\frac{\partial \tilde{x}}{\partial t} = D \frac{\partial^2 \tilde{x}}{\partial z^2} + f(\tilde{x}) \quad (6)$$

However for any discretization step h there exists a diffusion coefficient D , such that the discrete CNN model and the continuous PDE model present a different number of stable equilibrium points, i.e. they are not *topologically equivalent* (see Example 2 of Sec. 4 for a detailed study of this phenomenon). This is an example of a CNN that approximates a PDE, but does not converge to it, because it exhibits a qualitatively different dynamic behavior. Note that this is not contradicting the fact that if the diffusion coefficient D is fixed, then there exists a finite discretization step h and a CNN equation, that approximates and is *topologically equivalent* to the Nagumo equation.

These preliminary examples have shown some CNN equations that cannot be represented by any PDE, either because they do not approximate a PDE or because they are not topologically equivalent to it (i.e. they present a qualitatively different dynamic behavior). Such points will be investigated in the next section, where a significant class of canonical CNN equations is studied and the relationships between such a class and the corresponding PDE class are rigorously established.

3 On the relationship between CNNs and PDEs

The mathematical model of a canonical CNN equation, formally named Cellular Partial Difference Differential Equations (CPDDE), can be synthesized as reported in the following definition.

Definition 1 : A canonical CNN equation is a system of $N \times M$ nonlinear ODEs:

$$L(D_t)x_{ij}(t) = \sum_{(k,l) \in N_r(i,j)} T_{ij,kl}^A(x_{ij}, x_{kl})f(x_{kl}) + \sum_{(k,l) \in N_r(i,j)} T_{ij,kl}^B(u_{ij}, u_{kl})u_{kl} + \sum_{(k,l) \in N_r(i,j)} T_{ij,kl}^C(x_{ij}, x_{kl})x_{kl} + z_{ij} \quad (7)$$

The state variables x_{ij} are assumed to be arranged on a regular rectangular grid and are denoted by two indexes ($1 \leq i \leq N$, $1 \leq j \leq M$); $f(\cdot)$ is a $C^\infty(R)$ nonlinear function and represents the output;

u_{ij} is the input; z_{ij} is a constant bias term; $L(D_t)$ is a polynomial function of the differential operator $D_t = d/dt$; $T_{ij,kl}^A(x_{ij}, x_{kl})$ and $T_{ij,kl}^C(x_{ij}, x_{kl})$ are the output and the state feedback templates, that in general might be space-variant nonlinear functions of the state variables x_{ij} and x_{kl} ; $T_{ij,kl}^B(u_{ij}, u_{kl})$ is the input template; $N_r(i, j)$ denotes the neighborhood of interaction of each state-variable x_{ij} . The model is completed by specifying the *initial conditions*, i.e. $x_{ij}(0)$ and the space *boundary conditions*.

Note that Eq. (7) may contain higher order time derivatives, whereas multi-layer templates are not allowed.

For the sake of the simplicity, hereafter we assume that the boundary conditions be null or zero-flux and that the templates above T^A and T^C be linear and space-invariant; the inputs u_{ij} and the constant z_{ij} are assumed to be null as well. Under such assumptions, Eqs. (7) with the associated initial conditions yield:

$$\begin{aligned} L(D_t)x_{ij}(t) &= \sum_{|n|\leq r, |m|\leq r} T_{nm}^A f(x_{i+n, j+m}) + \sum_{|n|\leq r, |m|\leq r} T_{nm}^C x_{i+n, j+m} \quad (1 \leq i \leq N, \quad 1 \leq j \leq M) \\ x_{i,j}(0) &= x_{0ij} \quad (1 \leq i \leq N, \quad 1 \leq j \leq M) \end{aligned} \quad (8)$$

where r denotes the neighborhood radius and x_{0ij} denote arbitrary initial conditions.

Definition 2 : We introduce the set of associated PDEs that formally corresponds to Eqs. (8). The two space variables are denoted with z and w and are defined on a rectangular domain ($0 \leq z \leq l_z$; $0 \leq w \leq l_w$). The equations (with the associated initial conditions) are reported below:

$$\begin{aligned} L(D_t)\tilde{x}(z, w, t) &= L_A(D_z, D_w) f[\tilde{x}(z, w, t)] + L_C(D_z, D_w) \tilde{x}(z, w, t) \quad (0 \leq z \leq l_z; \quad 0 \leq w \leq l_w) \\ \tilde{x}(z, w, 0) &= \tilde{x}_0(z, w) \quad (0 \leq z \leq l_z; \quad 0 \leq w \leq l_w) \end{aligned} \quad (9)$$

where $\tilde{x}(z, w, t)$ is assumed to be a C^∞ function of the three variables z , w and t ; $L_A(D_z, D_w)$ and $L_C(D_z, D_w)$ are non-constant polynomial functions of the two space differential operators $D_z = \partial/\partial z$ and $D_w = \partial/\partial w$; $\tilde{x}_0(z, w)$ is a C^∞ function of the two space variables z and w ; $f(\cdot)$ is the C^∞ function defined in (7).

Definition 3 : The vector $\bar{x}_{ij}(t)$ is defined as follows:

$$\bar{x}_{ij}(t) = \tilde{x}(i h_z, j h_w, t) \quad h_z = \frac{l_z}{N}; \quad h_w = \frac{l_w}{M}; \quad (1 \leq i \leq N, \quad 1 \leq j \leq M) \quad (10)$$

where h_z and h_w are the two space discretization steps.

Remark : Note that we are dealing with three state variables $x_{ij}(t)$, i.e. the CNN state, $\tilde{x}(z, w, t)$, i.e. the PDE state, and $\bar{x}_{ij}(t)$, i.e. the state of the system obtained through PDE space discretization.

In order to study the relationship between canonical CNN equations and PDE models, we assume that Eq. (8) describes space-time phenomena, occurring in the same domain in which the PDE model is defined, i.e. ($0 \leq z \leq l_z$; $0 \leq w \leq l_w$). Therefore the templates T^A and T^C should depend on the space discretization steps $h_z = l_z/N$ and $h_w = l_w/M$; we assume that they are polynomial functions of the variables $1/h_z$ and $1/h_w$ (if this is not the case we assume that they can be approximated to any accuracy through a Taylor polynomial).

Remark : The choice of $1/h_z$ and $1/h_w$ as polynomial variables for approximating T^A and T^C can be motivated by observing that $1/h_z$ and $1/h_w$ means: *per unit length* (e.g. gain per unit length).

Definition 4 : The norm of a vector defined on a rectangular grid g , $\mathbf{v} = \{v_{ij}, (1 \leq i \leq N; 1 \leq j \leq M)\}$ is defined as:

$$\|\mathbf{v}\|_g = \sup_{i,j} |v_{ij}| \quad (11)$$

Definition 5 : A canonical CNN equation described by Eq. (8) approximates a PDE model described by Eq. (9) if and only if there exist two space differential operators $L_A(D_z, D_w)$ and $L_C(D_z, D_w)$ such that

$$\forall t : \lim_{(h_z, h_w) \rightarrow (0,0)} \|\mathbf{\Delta}(t)\|_g = 0 \quad (12)$$

where

$$\begin{aligned} \mathbf{\Delta}(t) &= \{\Delta_{ij}(t) = \Gamma_{ij}(t) - \Psi_{ij}(t), (1 \leq i \leq N; 1 \leq j \leq M)\} \\ \Gamma_{ij}(t) &= \sum_{|n| \leq r, |m| \leq r} T_{mn}^A f\{\tilde{x}[(i+n)h_z, (j+m)h_w, t]\} + \sum_{|n| \leq r, |m| \leq r} T_{mn}^C \tilde{x}[(i+n)h_z, (j+m)h_w, t] \\ \Psi_{ij}(t) &= L_A(D_z, D_w) f\{\tilde{x}[ih_z, jh_w, t]\} + L_C(D_z, D_w) \tilde{x}[ih_z, jh_w, t] \end{aligned} \quad (13)$$

We remark that if for $(h_z, h_w) \rightarrow (0,0)$ the two polynomials L_A and L_C reduce to constants, then the corresponding PDE (9) reduces to a set of uncoupled ODEs.

Definition 6 : A canonical CNN equation, described by Eq. (8) is *topologically equivalent* to a PDE model, described by Eq. (9), for given space discretization steps h_z and h_w , if there exists a C^0 -diffeomorphism $g(\cdot)$ such that

$$g[\mathbf{\Phi}_{t_1}(\bar{\mathbf{x}}_0)] = \bar{\mathbf{\Phi}}_{t_2}[g(\bar{\mathbf{x}}_0)] \quad (14)$$

where $\bar{\mathbf{x}}_0 = \{\bar{x}_{ij}(0), (1 \leq i \leq N; 1 \leq j \leq M)\}$; $\mathbf{\Phi}_{t_1}$ denotes the trajectory $\mathbf{x}(t_1) = \{x_{ij}(t_1), (1 \leq i \leq N; 1 \leq j \leq M)\}$ of the system (8), at time instant $t = t_1$, starting from the initial condition $\bar{\mathbf{x}}_0$; $\bar{\mathbf{\Phi}}_{t_2}$ denotes the trajectory $\bar{\mathbf{x}}(t_2) = \{\bar{x}_{ij}(t_2), (1 \leq i \leq N; 1 \leq j \leq M)\}$, of the discretized system defined in (10), at time instant $t = t_2$ and starting from the initial condition $g(\bar{\mathbf{x}}_0)$.

Definition 6 implies that the two systems (8) and (9) should exhibit the following properties, for given space discretization steps h_z and h_w :

- If the nonlinear PDE defined by (9) admits of a unique stable steady-state solution (attractor) for all the possible initial conditions $\tilde{x}(z, w, 0) = \tilde{x}_0(z, w)$, then the corresponding canonical CNN equation (8) presents a single stable attractor for all the possible initial conditions $x_{ij}(0)$.
- If the nonlinear PDE defined by (9) exhibits the following set of S stable steady-state solutions (attractors) $\bar{\mathcal{A}} = \{\bar{\mathcal{A}}_1, \dots, \bar{\mathcal{A}}_S\}$, then the canonical CNN equation (8) should present a set of attractors \mathcal{A} that is in a one-to-one correspondence with $\bar{\mathcal{A}}$, i.e $\mathcal{A} = \{\mathcal{A}_1, \dots, \mathcal{A}_S\}$.

The above consideration suggests the following procedure for verifying the *topological equivalence*:

Algorithm 1 : Let (8) be a canonical CNN equation, described by the template $T^A(h_z, h_w)$ and $T^C(h_z, h_w)$, that approximates the PDE model (9) for $(h_z, h_w) \rightarrow (0,0)$. For finite values of the space discretization steps $h_z = \bar{h}_z$ and $h_w = \bar{h}_w$, the *topological equivalence* between the two models can be verified according to the following two steps:

1. Check that there exists $\varepsilon > 0$ such that the canonical CNN equation (8) does not exhibit any bifurcation phenomena for $0 < h_z < \varepsilon$, $0 < h_w < \varepsilon$.
2. Check that the canonical CNN equation (8) does not present bifurcations for $0 < h_z < \bar{h}_z + \varepsilon$, $0 < h_w < \bar{h}_w + \varepsilon$.

Note that the above points require to verify that, for a given range of the parameters h_z and h_w , the canonical CNN equation does not present either local or global bifurcations. The local bifurcation analysis can be carried out by examining the invariant limit sets of the system for $(h_z, h_w) \rightarrow 0$ (i.e. equilibrium points, limit cycles, non-periodic attractors); hence by studying their local properties,

i.e. the equilibrium point eigenvalues and the limit cycle Floquet's multipliers. The global bifurcation analysis is more difficult and could become a formidable task because it would require to determine the stable and the unstable manifolds of the invariant limit sets. The bifurcation analysis for the case of the discrete Nagumo equation is developed in Example 2 of Sec. 4.

Definition 7 : A canonical CNN equation, described by the template $T^A(h_z, h_w)$ and $T^C(h_z, h_w)$ is *equivalent* to a PDE model, for finite values of $h_z = \bar{h}_z$ and $h_w = \bar{h}_w$, if and only if the canonical CNN equation approximates the PDE model for $(h_z, h_w) \rightarrow (0, 0)$ and the two models are *topologically equivalent* for $h_z = \bar{h}_z$ and $h_w = \bar{h}_w$.

It is derived that if a canonical CNN equation and a PDE model are equivalent, they presents a similar dynamic behavior and exhibits the same qualitative spatio-temporal phenomena. If this is not the case, the two models in general presents a different dynamics.

4 Examples

In this section we consider some canonical CNN equations and we investigate the conditions that guarantee the equivalence to a PDE model, according to Definition 7. The equivalence will be studied by verifying that the canonical CNN equation approximates the PDE model (see Def. 5) and that the two models are topologically equivalent (see Def. 6).

Example 1 : Let us consider a linear canonical CNN equation, described by the following one-dimensional templates:

$$\begin{aligned} T^A &= 0 \\ T^C &= [r, p, s] \end{aligned} \tag{15}$$

As pointed out in the previous section, we assume that the template elements can be expanded in a Taylor series of the inverse of the space-step h_z . We also assume that the series can be truncated at a suitable order, hereafter denoted by L . Hence the template coefficients can be written as a L -th order polynomial function of the inverse of the space-step h_z (that, hereafter, for the sake of simplicity, will be denoted with h):

$$\begin{aligned} p &= p_0 + \frac{p_1}{h} + \frac{p_2}{h^2} + \frac{p_3}{h^3} + \dots + \frac{p_L}{h^L} \\ s &= s_0 + \frac{s_1}{h} + \frac{s_2}{h^2} + \frac{s_3}{h^3} + \dots + \frac{s_L}{h^L} \\ r &= r_0 + \frac{r_1}{h} + \frac{r_2}{h^2} + \frac{r_3}{h^3} + \dots + \frac{r_L}{h^L} \end{aligned} \tag{16}$$

Note that in the Taylor expansion above, the terms of the type h^α with α positive integer, are not considered because they vanish for $h \rightarrow 0$ and therefore do not play any role for the PDE approximation.

Such templates give rise to the following canonical CNN equation:

$$L(D_t)x_i(t) = p x_i(t) + s x_{i+1}(t) + r x_{i-1}(t) \quad (1 \leq i \leq N) \tag{17}$$

According to Def. 7, the equivalence between the above canonical CNN equation (17) and the corresponding PDE models is split in two sub-problems: the identification of the PDE models that are approximated by (17), according to Def. 5; the study of the topological equivalence, as defined in Def. 6.

Approximation: We present a general technique for investigating the approximation problem, that is valid for all the canonical CNN equations. Def. 5 requires to compute $\tilde{x}[(i+1)h]$ and $\tilde{x}[(i-1)h]$. They

can be computed through the Taylor series expansion of the PDE state variable $\tilde{x}(z, t)$ centered in $z = z_i = h$ i:

$$\begin{aligned}\tilde{x}(z_i + h, t) &= \tilde{x}(z_i, t) + \frac{\partial \tilde{x}}{\partial z}(z_i, t) h + \frac{\partial^2 \tilde{x}}{\partial z^2}(z_i, t) \frac{h^2}{2} + \frac{\partial^3 \tilde{x}}{\partial z^3}(z_i, t) \frac{h^3}{6} + \dots + \frac{\partial^K \tilde{x}}{\partial z^K}(\alpha_i, t) \frac{h^K}{K!} \\ &\hspace{15em} \alpha_i \in [z_i, z_i + h] \\ \tilde{x}(z_i - h, t) &= \tilde{x}(z_i, t) - \frac{\partial \tilde{x}}{\partial z}(z_i, t) h + \frac{\partial^2 \tilde{x}}{\partial z^2}(z_i, t) \frac{h^2}{2} - \frac{\partial^3 \tilde{x}}{\partial z^3}(z_i, t) \frac{h^3}{6} + \dots + \frac{\partial^K \tilde{x}}{\partial z^K}(\beta_i, t) \frac{(-h)^K}{K!} \\ &\hspace{15em} \beta_i \in [z_i - h, z_i]\end{aligned}\tag{18}$$

In order to evaluate $\Delta_i(t)$ (see Def. 5) one has to compute $\Gamma_i(t)$ and then to determine (if there exists) a differential space operator $L_C(D_z)$ such that Eq. (12) is satisfied. The quantity $\Gamma_i(t)$ can be computed by using the series expansion (18). We have:

$$\begin{aligned}\Gamma_i(t) &= p \tilde{x}(z_i, t) + s \tilde{x}(z_i + h, t) + r \tilde{x}(z_i - h, t) \\ &= (p + s + r) \tilde{x}(z_i, t) + (s - r) h \frac{\partial \tilde{x}}{\partial z}(z_i, t) + (s + r) \frac{h^2}{2} \frac{\partial^2 \tilde{x}}{\partial z^2}(z_i, t) + (s - r) \frac{h^3}{6} \frac{\partial^3 \tilde{x}}{\partial z^3}(z_i, t) + \dots \\ &\quad \dots + \frac{h^K}{K!} \left(s \frac{\partial^K \tilde{x}}{\partial z^K}(\alpha_i, t) + (-1)^K r \frac{\partial^K \tilde{x}}{\partial z^K}(\beta_i, t) \right)\end{aligned}\tag{19}$$

The terms of the above expression (19) are finite, as $h \rightarrow 0$, if and only if the template element coefficients satisfy the following conditions:

$$\begin{aligned}p_1 + s_1 + r_1 &= 0 & p_2 + s_2 + r_2 &= 0 \\ s_2 - r_2 &= 0 & p_k = s_k = r_k &= 0 \quad (k \geq 3)\end{aligned}\tag{20}$$

Therefore $\Gamma_i(t)$, by use of (19), (20) and of (16), can be written as:

$$\begin{aligned}\Gamma_i(t) &= (p_0 + s_0 + r_0) \tilde{x}(z_i, t) + (s_0 - r_0) h \frac{\partial \tilde{x}}{\partial z}(z_i, t) + (s_1 - r_1) \frac{\partial \tilde{x}}{\partial z}(z_i, t) \\ &\quad + (s_0 + r_0) \frac{h^2}{2} \frac{\partial^2 \tilde{x}}{\partial z^2}(z_i, t) + \frac{s_1 + r_1}{2} h \frac{\partial^2 \tilde{x}}{\partial z^2}(z_i, t) + \frac{s_2 + r_2}{2} \frac{\partial^2 \tilde{x}}{\partial z^2}(z_i, t) \\ &\quad + \frac{h^3}{6} \left[\left(s_0 + \frac{s_1}{h} + \frac{s_2}{h^2} \right) \frac{\partial^3 \tilde{x}}{\partial z^3}(\alpha_i, t) - \left(r_0 + \frac{r_1}{h} + \frac{r_2}{h^2} \right) \frac{\partial^3 \tilde{x}}{\partial z^3}(\beta_i, t) \right]\end{aligned}\tag{21}$$

The above expression allows to identify the space differential operator $L_C(D_z)$. We have:

$$L_C(D_z)[\tilde{x}(z, t)] = (p_0 + s_0 + r_0) \tilde{x}(z, t) + (s_1 - r_1) \frac{\partial \tilde{x}}{\partial z}(z, t) + \frac{s_2 + r_2}{2} \frac{\partial^2 \tilde{x}}{\partial z^2}(z, t)\tag{22}$$

By use of (21) and of (22), the quantity $\Delta_i(t)$, reported in Def. 5, is readily computed as:

$$\begin{aligned}\Delta_i(t) &= (s_0 - r_0) h \frac{\partial \tilde{x}}{\partial z}(z_i, t) + (s_0 + r_0) \frac{h^2}{2} \frac{\partial^2 \tilde{x}}{\partial z^2}(z_i, t) + \frac{s_1 + r_1}{2} h \frac{\partial^2 \tilde{x}}{\partial z^2}(z_i, t) \\ &\quad + \frac{h^3}{6} \left[\left(s_0 + \frac{s_1}{h} + \frac{s_2}{h^2} \right) \frac{\partial^3 \tilde{x}}{\partial z^3}(\alpha_i, t) - \left(r_0 + \frac{r_1}{h} + \frac{r_2}{h^2} \right) \frac{\partial^3 \tilde{x}}{\partial z^3}(\beta_i, t) \right]\end{aligned}\tag{23}$$

Since the function $\tilde{x}(z, t)$ has been assumed to be C^∞ , its derivatives are bounded for each z_i ; hence we derive:

$$\forall t, i : \quad \lim_{h \rightarrow 0} |\Delta_i(t)| = 0, \quad (24)$$

that according to Defs. 4 and 5 yields:

$$\forall t : \quad \lim_{h \rightarrow 0} \|\mathbf{\Delta}(t)\|_g = 0 \quad (25)$$

The following considerations hold:

1. The result above (25) shows that if the conditions (20) are matched then the canonical CNN equation (17) **approximates** the following PDE for $h \rightarrow 0$:

$$L(D_t)[\tilde{x}(z, t)] = (p_0 + s_0 + r_0) \tilde{x}(z, t) + (s_1 - r_1) \frac{\partial \tilde{x}}{\partial z}(z, t) + \frac{s_2 + r_2}{2} \frac{\partial^2 \tilde{x}}{\partial z^2}(z, t) \quad (26)$$

We note that, if the space differential operator $L_C(D_z)$ is a constant polynomial (for instance if $p = p_0, s = s_0, r = r_0$), the canonical CNN equation reduces to a set of uncoupled ODEs, that is of no interest in this study.

2. If the conditions (20) are not satisfied, then the canonical CNN equation (17) **does not approximate** any PDE, for $h \rightarrow 0$.

Topological equivalence: Let us assume that the conditions (20) are fulfilled, i.e. the canonical CNN equation (17) *approximates* the PDE model (26), according to Def. 5. An autonomous linear system may present only two dynamic behaviors (with the exception of a set of parameters of measure zero): a) stability, which implies the existence of a single attractor (globally stable equilibrium point); b) instability, in case each trajectory (with the exception of a set of measure zero) diverges. In the following we assume that the linear PDE model (26) be stable.

According to Def. 6, the *topological equivalence* is defined for a finite value of the space discretization step h . For stable systems the check of the *topological equivalence* simply require to verify that the ODE, described by (17) be stable, i.e. that all the system eigenvalues have negative real part.

In the particular case $L(D_t) = \partial/\partial t$, the explicit computation of the eigenvalues yields the following stability conditions

$$\mathbf{Re}[\lambda_i] = \mathbf{Re}[p + 2\sqrt{rs} \cos\left(\frac{i\pi}{N+1}\right)] < 0, \quad (1 \leq i \leq N) \quad (27)$$

where $N = l_z/h$, according to (10).

It is derived that if $L(D_t) = \partial/\partial t$ and the linear PDE model is stable, then such a model is equivalent to the canonical CNN equation (17), for a given space discretization step h , if and only if both the approximation (20) and the stability conditions above (27) are satisfied. If this is not the case, the canonical CNN equation (17) is not equivalent to the PDE (26).

Example 2 : Let us consider a nonlinear canonical CNN equation, described by the following one-dimensional templates:

$$\begin{aligned} T^A &= [r^A \ p^A \ s^A] \\ T^C &= [r^C, \ p^C, \ s^C] \end{aligned} \quad (28)$$

with

$$\begin{aligned} p^{A,C} &= p_0^{A,C} + \frac{p_1^{A,C}}{h} + \frac{p_2^{A,C}}{h^2} + \frac{p_3^{A,C}}{h^3} + \dots + \frac{p_L^{A,C}}{h^L} \\ s^{A,C} &= s_0^{A,C} + \frac{s_1^{A,C}}{h} + \frac{s_2^{A,C}}{h^2} + \frac{s_3^{A,C}}{h^3} + \dots + \frac{s_L^{A,C}}{h^L} \\ r^{A,C} &= r_0^{A,C} + \frac{r_1^{A,C}}{h} + \frac{r_2^{A,C}}{h^2} + \frac{r_3^{A,C}}{h^3} + \dots + \frac{r_L^{A,C}}{h^L} \end{aligned} \quad (29)$$

The following canonical CNN equation is obtained:

$$L(D_t)x_i(t) = p^A f[x_i(t)] + s^A f[x_{i+1}(t)] + r^A f[x_{i-1}(t)] + p^C x_i(t) + s^C x_{i+1}(t) + r^C x_{i-1}(t) \quad (1 \leq i \leq N) \quad (30)$$

Approximation: Since the nonlinear function $f(\cdot)$ has been assumed to be C^∞ , it admits of a Taylor expansion. By proceeding as in Example 1, it is derived that the canonical CNN equation (30) approximates a PDE if and only if the following constraints are fulfilled:

$$\begin{aligned} p_1^{A,C} + s_1^{A,C} + r_1^{A,C} &= 0 & p_2^{A,C} + s_2^{A,C} + r_2^{A,C} &= 0 \\ s_2^{A,C} - r_2^{A,C} &= 0 & p_k^{A,C} = s_k^{A,C} = r_k^{A,C} &= 0 \quad (k \geq 3) \end{aligned} \quad (31)$$

The corresponding PDE is:

$$\begin{aligned} L(D_t)[\tilde{x}(z, t)] &= (p_0^A + s_0^A + r_0^A) f[\tilde{x}(z, t)] + (s_1^A - r_1^A) \frac{\partial f[\tilde{x}(z, t)]}{\partial z} + \frac{s_2^A + r_2^A}{2} \frac{\partial^2 f[\tilde{x}(z, t)]}{\partial z^2} \\ &+ (p_0^C + s_0^C + r_0^C) \tilde{x}(z, t) + (s_1^C - r_1^C) \frac{\partial \tilde{x}}{\partial z}(z, t) + \frac{s_2^C + r_2^C}{2} \frac{\partial^2 \tilde{x}}{\partial z^2}(z, t) \end{aligned} \quad (32)$$

Topological equivalence: Since the canonical CNN equation (30) is nonlinear, the study of the *topological equivalence*, according to Def. 6 and Algorithm 1, is more complex.

We restrict our attention to the well known case of the Nagumo equation, studied by in [Keener, 1987]:

$$\frac{\partial \tilde{x}}{\partial t} = D \frac{\partial^2 \tilde{x}}{\partial z^2} + f(\tilde{x}) \quad (33)$$

where D is the diffusion coefficient. We assume zero-flux boundary conditions, i.e.

$$\frac{\partial \tilde{x}}{\partial z} \Big|_{z=0,l} = 0 \quad (34)$$

Such an equation corresponds to the PDE and the canonical CNN equation (32) and (30) respectively, by assuming $L(D_t) = D_t$ and, in addition to (31), the following constraints:

$$\begin{aligned} p_0^A + s_0^A + r_0^A &= 1 & s_1^A = s_2^A = r_1^A = r_2^A &= 0 \\ p_0^C + s_0^C + r_0^C &= 0 & s_1^C = r_1^C &= 0 \\ \frac{s_2^C + r_2^C}{2} &= D \end{aligned} \quad (35)$$

We also suppose that the nonlinear function $f(\cdot)$ can be approximated by the following expression (for $0 \leq \alpha \leq 0.5$).

$$f(\tilde{x}) = \begin{cases} -\alpha \tilde{x} & \tilde{x} \leq 0 \\ -\tilde{x}^3 + (1 + \alpha)\tilde{x}^2 - \alpha \tilde{x} & 0 \leq \tilde{x} \leq 1 \\ (1 - \alpha)(\tilde{x} - 1) & \tilde{x} \geq 1 \end{cases} \quad (36)$$

The above function is continuous with its first-order derivative; it coincides with the cubic function considered in [Keener, 1987] for $0 \leq \tilde{x} \leq 1$, whereas it is linear for $|\tilde{x}| > 1$. The latter property allows to simplify the numerical computation of the bifurcation processes occurring in the corresponding

canonical CNN equation. For sake of completeness such a CNN model, with the corresponding zero-flux boundary conditions, is reported below:

$$\begin{aligned}\frac{dx_1(t)}{dt} &= \frac{D}{h^2} [x_2(t) - x_1(t)] + f[x_1(t)] \\ \frac{dx_i(t)}{dt} &= \frac{D}{h^2} [x_{i+1}(t) - 2x_i(t) + x_{i-1}(t)] + f[x_i(t)] \quad (2 \leq i \leq N-1) \\ \frac{dx_N(t)}{dt} &= \frac{D}{h^2} [x_{N-1}(t) - x_N(t)] + f[x_N(t)]\end{aligned}\tag{37}$$

We denote with $h_D = \frac{h}{\sqrt{D}}$ the space discretization step, normalized with respect to \sqrt{D} . The analysis of the dynamic system described by (37) yields the following results:

1. For any number N of cells, there exists h_D^* such that for $0 \leq h_D < h_D^*$ the canonical CNN equation (37) presents only three equilibrium points:
 - (a) two stable equilibrium points $P_a = (0, 0, \dots, 0, 0)$ and $P_b = (1, 1, \dots, 1, 1)$, whose Jacobian matrix exhibits N negative real eigenvalues;
 - (b) one unstable equilibrium point $P = (\alpha, \alpha, \dots, \alpha, \alpha)$ that presents one positive real eigenvalues.

This implies, according to Algorithm 1, that for each finite values of $h_D < h_D^*$ the canonical CNN equation (37) and the PDE (33) models are *topologically equivalent*. Since we have already shown that (37) approximates (33), then for $h_D \leq h_D^*$ the two models are *equivalent*, according to Def. 7.

2. If $h_D \geq h_D^*$, then the system (37) still presents the two stable equilibrium points P_a and P_b . The unstable point $P = (\alpha, \alpha, \dots, \alpha, \alpha)$ undergoes a series of pitchfork bifurcations, that finally gives rise to the emergence of a number of additional stable equilibrium points. The bifurcation process is studied in detail for some selected values of N : we will show that the main characteristics are not influenced by the number of cells.
 - (a) Figure 2 shows the main bifurcation phenomena for $N = 4$ and $\alpha = 0.5$. The bifurcation process can be described as follows.
 - i. For $h_D < h_D^* = 1.531$ the equilibrium point $P = (\alpha, \alpha, \alpha, \alpha)$ is a saddle point of index one (i.e. it presents only one positive real eigenvalue).
 - ii. For $h_D = h_D^* = 1.531$ a pitchfork bifurcation gives rise to the birth of two additional saddle points of index one (denoted with P_1 and P_2 respectively); as a consequence of the pitchfork bifurcation the original equilibrium point P becomes a saddle point of index two.
 - iii. The two points P_1 and P_2 undergo a pitchfork bifurcation for $h_D = h_D^S = 2.378$. As a result of the bifurcation the two points P_1 and P_2 become stable nodes (i.e. with all negative real eigenvalues) and four saddle points of index one emerge (denoted with P_{11} , P_{12} and P_{21} , P_{22} respectively.) It is worth noting that by increasing h_D the two stable nodes P_1 and P_2 do not undergo further bifurcations and converge to the equilibrium points $(0, 0, 1, 1)$ and $(1, 1, 0, 0)$ respectively of the uncoupled network.
 - iv. The point $P = (\alpha, \alpha, \alpha, \alpha)$ presents a series of additional pitchfork bifurcation: the first one is reported in Fig. 2 and occurs for $h_D = 2.829$. The bifurcation gives rise to the birth of two saddle points of index two (denoted with P_3 and P_4 respectively), whereas the point P becomes a saddle point of index 3.

- (b) Figure 3 shows the case $N = 10$ and $\alpha = 0.5$. The bifurcation process can be described as follows.
- i. For $h_D < h_D^* = 0.6258$ the equilibrium point $P = (\alpha, \dots, \alpha)$ is a saddle point of index one: its index is denoted with I_P . Then the point P undergoes a series of pitchfork bifurcation. The effect of each bifurcation is to increase by one the index I_P of point P and to create two additional saddles of index I_P . The first two bifurcations, reported in Fig. 3, occurs for $h_D = h_D^* = 0.6258$ and $h_D = 1.2361$; the emerging saddles are denoted with P_1, P_2, P_3 , and P_4 respectively.
 - ii. For $h_D = h_D^S = 1.5288$. i.e. after the second bifurcation of P , the two saddles P_1 and P_2 undergo a pitchfork bifurcation. As a result they become stable nodes and give birth to four saddles of index one (denoted as P_{11}, P_{12} and P_{21}, P_{22} respectively.) As in the case $N = 4$ by increasing h_D the two stable nodes P_1 and P_2 do not undergo further bifurcations and converge to the equilibrium points $(0, 0, 0, 0, 0, 1, 1, 1, 1, 1)$ and $(1, 1, 1, 1, 1, 0, 0, 0, 0, 0)$ of the uncoupled network.
- (c) Figure 4 shows the case $N = 20$ and $\alpha = 0.5$. We can observe the same bifurcation process described for 10 cells.
- i. The saddle point $P = (\alpha, \dots, \alpha)$ (of initial index $I_P = 1$, for $h_D < h_D^* = 0.3139$) exhibits a sequence of pitchfork bifurcations; at each bifurcation the index I_P increases by one and two saddles of index I_P emerge. The first three bifurcations are shown in Fig. 4. They occur for $h_D = 0.3139, h_D = 0.6258$ and $h_D = 0.9338$. The saddles are denoted with P_1, \dots, P_6 respectively.
 - ii. For $h_D = h_D^S = 1.1190$. i.e. after the third bifurcation of P , the two saddles P_1 and P_2 undergo a pitchfork bifurcations and become stable nodes. By increasing h_D they converge to the equilibrium points of the uncoupled network represented by a sequence of ten zeros (ones) and ten ones (zeros) respectively.
- (d) For larger value of N the bifurcation process can still be described according to the following two considerations:
- i. The saddle point $P = (\alpha, \dots, \alpha)$ undergoes a series of pitchfork bifurcation, that give rise to the increment of its index I_P and to the birth of two new saddles of index I_P . Note that by increasing h_D the point $P = (\alpha, \dots, \alpha)$ becomes an unstable node (i.e. with all positive real eigenvalues). Note also that the normalized discretization step h_D^* corresponding to the first bifurcation decreases as the number of cells N increases.
 - ii. The first couple of stable nodes emerges as a consequence of a pitchfork bifurcation of the first two saddles that bifurcate from $P = (\alpha, \dots, \alpha)$.

As a result of the above study we can claim that the canonical CNN equation is not *topologically equivalent* to the PDE model for $h_D \geq h_D^*$, i.e. after the occurrence of the first bifurcation. In addition for $h_D > h_D^S$ the discrete canonical CNN equation presents a pair of stable equilibrium points that are not present in the original PDE, i.e. there is not a one-to-one correspondence between the attractors of the two models.

3. For any number N of cells and diffusion coefficient D , there exists h_D^F such that for $h_D > h_D^F$ the cells can be considered uncoupled, i.e. there is a one-to-one correspondence between the set of equilibrium points of the dynamical system (37) and the set of equilibrium points of N uncoupled cells. Each uncoupled cell x_i presents two stable equilibrium points $P_a^i = 0$ and $P_b^i = 1$ and one unstable point $P^i = \alpha$. It is derived that for $h_D > h_D^F$ the whole system possesses 2^N stable equilibrium points (with all negative real eigenvalues) and $3^N - 2^N$ unstable equilibrium points (with at least one positive real eigenvalue).

In order to show a numerical example of the complete bifurcation process, we have considered a CNN structure composed by 10 cells and we have determined the number of stable equilibrium points as a function of the normalized discretization step h_D . The results can be summarized as follows (they are reported in Fig. 5)

- (a) For $0 < h_D < h_D^S = 1.5288$ the canonical CNN equation exhibits only two stable equilibrium points i.e. the origin and the point whose coordinates are all 1. This is in agreement with the detailed bifurcation analysis shown in Fig. 3.
- (b) For $h_D > 1.5288$ two additional stable equilibrium points emerge; they correspond to the points denoted with P_1 and P_2 in Fig. 3.
- (c) By further increasing h new stable equilibrium points emerges, through pitchfork bifurcations, that are not shown in Fig. 3; finally, for $h_D > h_D^F = 5.47$ the cells behave as they were uncoupled, i.e. each cell exhibits two stable equilibrium points, giving rise to a total number of $2^{10} = 1024$ equilibrium points.

Remark: According to the discussion above and to Def. 6, the propagation failure phenomenon, studied in [Keener, 1987; Perez-Munuzuri *et al.*, 1993], occurs for those $h_D > h_D^S$ such that there is not a one-to-one correspondence between the stable equilibrium points of the two models. The statement in [Keener, 1987] regarding the existence of propagation failure for arbitrarily small space discretization steps h , can be reformulated as follows: for each discretization step h (even arbitrarily small) there exists a diffusion coefficient D such that $h_D = \frac{h}{\sqrt{D}} > h_D^S$, i.e. the canonical CNN equation and the PDE model are not *topologically equivalent*.

Example 3 : Let us consider the linear canonical CNN equation, described by the following one-dimensional templates:

$$\begin{aligned} T^A &= 0 \\ T^C &= [v, r, p, s, q] \end{aligned} \tag{38}$$

with

$$\begin{aligned} p &= p_0 + \frac{p_1}{h} + \frac{p_2}{h^2} + \frac{p_3}{h^3} + \dots + \frac{p_L}{h^L} \\ s &= s_0 + \frac{s_1}{h} + \frac{s_2}{h^2} + \frac{s_3}{h^3} + \dots + \frac{s_L}{h^L} \\ r &= r_0 + \frac{r_1}{h} + \frac{r_2}{h^2} + \frac{r_3}{h^3} + \dots + \frac{r_L}{h^L} \\ q &= q_0 + \frac{q_1}{h} + \frac{q_2}{h^2} + \frac{q_3}{h^3} + \dots + \frac{q_L}{h^L} \\ v &= v_0 + \frac{v_1}{h} + \frac{v_2}{h^2} + \frac{v_3}{h^3} + \dots + \frac{v_L}{h^L} \end{aligned} \tag{39}$$

The corresponding canonical CNN equation is reported below:

$$L(D_t)x_i(t) = p x_i(t) + s x_{i+1}(t) + r x_{i-1}(t) + q x_{i+2}(t) + v x_{i-2}(t) \quad (1 \leq i \leq N) \tag{40}$$

Approximation: In order to apply the technique shown in Example 1, the explicit Taylor expansions

of $\tilde{x}[(i+2)h, t] = \tilde{x}(z_i + 2h, t)$ and $\tilde{x}[(i-2)h, t] = \tilde{x}(z_i - 2h, t)$ should be evaluated. We have:

$$\begin{aligned}\tilde{x}(z_i + 2h, t) &= \tilde{x}(z_i, t) + \frac{\partial \tilde{x}}{\partial z}(z_i, t) 2h + \frac{\partial^2 \tilde{x}}{\partial z^2}(z_i, t) \frac{2^2 h^2}{2} + \frac{\partial^3 \tilde{x}}{\partial z^3}(z_i, t) \frac{2^3 h^3}{6} + \dots + \frac{\partial^K \tilde{x}}{\partial z^K}(\gamma_i, t) \frac{2^K h^K}{K!} \\ &\quad \gamma_i \in [z_i, z_i + 2h] \\ \tilde{x}(z_i - 2h, t) &= \tilde{x}(z_i, t) - \frac{\partial \tilde{x}}{\partial z}(z_i, t) 2h + \frac{\partial^2 \tilde{x}}{\partial z^2}(z_i, t) \frac{2^2 h^2}{2} - \frac{\partial^3 \tilde{x}}{\partial z^3}(z_i, t) \frac{2^3 h^3}{6} + \dots + \frac{\partial^K \tilde{x}}{\partial z^K}(\delta_i, t) \frac{(-2h)^K}{K!} \\ &\quad \delta_i \in [z_i - 2h, z_i]\end{aligned}\tag{41}$$

The quantity $\Gamma_i(t)$ can be computed by using the series expansion (18) and (41). We have:

$$\begin{aligned}\Gamma_i(t) &= p \tilde{x}(z_i, t) + s \tilde{x}(z_i + h, t) + r \tilde{x}(z_i - h, t) + q \tilde{x}(z_i + 2h, t) + v \tilde{x}(z_i - 2h, t) \\ &= (p + s + r + q + v) \tilde{x}(z_i, t) + [s - r + 2(q - v)] h \frac{\partial \tilde{x}}{\partial z}(z_i, t) + [s + r + 2^2(q + v)] \frac{h^2}{2} \frac{\partial^2 \tilde{x}}{\partial z^2}(z_i, t) \\ &\quad + [s - r + 2^3(q - v)] \frac{h^3}{6} \frac{\partial^3 \tilde{x}}{\partial z^3}(z_i, t) + [s + r + 2^4(q + v)] \frac{h^4}{24} \frac{\partial^4 \tilde{x}}{\partial z^4}(z_i, t) + \dots \\ &\quad \dots + \frac{h^K}{K!} \left[s \frac{\partial^K \tilde{x}}{\partial z^K}(\alpha_i, t) + (-1)^K r \frac{\partial^K \tilde{x}}{\partial z^K}(\beta_i, t) + 2^K q \frac{\partial^K \tilde{x}}{\partial z^K}(\gamma_i, t) + (-2)^K v \frac{\partial^K \tilde{x}}{\partial z^K}(\delta_i, t) \right]\end{aligned}\tag{42}$$

By imposing that the coefficients of the above expression (42) be finite for $h \rightarrow 0$, the following constraints are obtained:

$$\begin{aligned}p_k + s_k + r_k + q_k + v_k &= 0 \quad (1 \leq k \leq 4) \\ s_k - r_k + 2(q_k - v_k) &= 0 \quad (2 \leq k \leq 4) \\ s_k + r_k + 2^2(q_k + v_k) &= 0 \quad (3 \leq k \leq 4) \\ s_k - r_k + 2^3(q_k - v_k) &= 0 \quad (k = 4) \\ p_k = s_k = r_k = q_k = v_k &= 0 \quad (k \geq 5)\end{aligned}\tag{43}$$

By computing, as in Example 1, the quantity Δ_i (see Def. 5) we obtain that, if Eqs. (43) are fulfilled, the canonical CNN equation approximates the following PDE for $h \rightarrow 0$:

$$\begin{aligned}L(D_t)[\tilde{x}(z, t)] &= (p_0 + s_0 + r_0 + q_0 + v_0) \tilde{x}(z, t) + [s_1 - r_1 + 2(q_1 - v_1)] \frac{\partial \tilde{x}}{\partial z}(z, t) \\ &\quad + \frac{s_2 + r_2 + 2^2(q_2 + v_2)}{2} \frac{\partial^2 \tilde{x}}{\partial z^2}(z, t) + \frac{s_3 - r_3 + 2^3(p_3 - v_3)}{6} \frac{\partial^3 \tilde{x}}{\partial z^3}(z, t) \\ &\quad + \frac{s_4 + r_4 + 2^4(q_4 + v_4)}{24} \frac{\partial^4 \tilde{x}}{\partial z^4}(z, t)\end{aligned}\tag{44}$$

If Eqs. (43) are not satisfied the canonical CNN equation does not approximate any PDE model and hence does not converge to any PDE.

Topological equivalence: Since the model is linear, the considerations of Example 1 apply.

Example 4 : Let us consider the nonlinear canonical CNN equation, described by the following one-dimensional templates:

$$\begin{aligned}T^A &= [v^A, r^A, p^A, s^A, q^A] \\ T^C &= [v^C, r^C, p^C, s^C, q^C]\end{aligned}\tag{45}$$

with

$$\begin{aligned}
p^{A,C} &= p_0^{A,C} + \frac{p_1^{A,C}}{h} + \frac{p_2^{A,C}}{h^2} + \frac{p_3^{A,C}}{h^3} + \dots + \frac{p_L^{A,C}}{h^L} \\
s^{A,C} &= s_0^{A,C} + \frac{s_1^{A,C}}{h} + \frac{s_2^{A,C}}{h^2} + \frac{s_3^{A,C}}{h^3} + \dots + \frac{s_L^{A,C}}{h^L} \\
r^{A,C} &= r_0^{A,C} + \frac{r_1^{A,C}}{h} + \frac{r_2^{A,C}}{h^2} + \frac{r_3^{A,C}}{h^3} + \dots + \frac{r_L^{A,C}}{h^L} \\
q^{A,C} &= q_0^{A,C} + \frac{q_1^{A,C}}{h} + \frac{q_2^{A,C}}{h^2} + \frac{q_3^{A,C}}{h^3} + \dots + \frac{q_L^{A,C}}{h^L} \\
v^{A,C} &= v_0^{A,C} + \frac{v_1^{A,C}}{h} + \frac{v_2^{A,C}}{h^2} + \frac{v_3^{A,C}}{h^3} + \dots + \frac{v_L^{A,C}}{h^L}
\end{aligned} \tag{46}$$

The following canonical CNN equation is derived:

$$\begin{aligned}
L(D_t)x_i(t) &= p^A f[x_i(t)] + s^A f[x_{i+1}(t)] + r^A f[x_{i-1}(t)] + q^A f[x_{i+2}(t)] + v^A f[x_{i-2}(t)] \\
&+ p^C x_i(t) + s^C x_{i+1}(t) + r^C x_{i-1}(t) + q^C x_{i+2}(t) + v^C x_{i-2}(t) \quad (1 \leq i \leq N)
\end{aligned} \tag{47}$$

Approximation: By proceeding as in the previous Example 3, we find that the canonical CNN equation (47) approximate a PDE if and only if the following constraints are fulfilled:

$$\begin{aligned}
p_k^{A,C} + s_k^{A,C} + r_k^{A,C} + q_k^{A,C} + v_k^{A,C} &= 0 \quad (1 \leq k \leq 4) \\
s_k^{A,C} - r_k^{A,C} + 2(q_k^{A,C} - v_k^{A,C}) &= 0 \quad (2 \leq k \leq 4) \\
s_k^{A,C} + r_k^{A,C} + 2^2(q_k^{A,C} + v_k^{A,C}) &= 0 \quad (3 \leq k \leq 4) \\
s_k^{A,C} - r_k^{A,C} + 2^3(q_k^{A,C} - v_k^{A,C}) &= 0 \quad (k = 4) \\
p_k^{A,C} = s_k^{A,C} = r_k^{A,C} = q_k^{A,C} = v_k^{A,C} &= 0 \quad (k \geq 5)
\end{aligned} \tag{48}$$

The corresponding PDE is:

$$\begin{aligned}
L(D_t)[\tilde{x}(z, t)] &= (p_0^A + s_0^A + r_0^A + q_0^A + v_0^A) f[\tilde{x}(z, t)] + [s_1^A - r_1^A + 2(q_1^A - v_1^A)] \frac{\partial f[\tilde{x}(z, t)]}{\partial z} \\
&+ \frac{s_2^A + r_2^A + 2^2(q_2^A + v_2^A)}{2} \frac{\partial^2 f[\tilde{x}(z, t)]}{\partial z^2} + \frac{s_3^A - r_3^A + 2^3(q_3^A - v_3^A)}{6} \frac{\partial^3 f[\tilde{x}(z, t)]}{\partial z^3} \\
&+ \frac{s_4^A + r_4^A + 2^4(q_4^A + v_4^A)}{24} \frac{\partial^4 f[\tilde{x}(z, t)]}{\partial z^4} \\
&+ (p_0^C + s_0^C + r_0^C + q_0^C + v_0^C) \tilde{x}(z, t) + [s_1^C - r_1^C + 2(q_1^C - v_1^C)] \frac{\partial \tilde{x}}{\partial z}(z, t) \\
&+ \frac{s_2^C + r_2^C + 2^2(q_2^C + v_2^C)}{2} \frac{\partial^2 \tilde{x}}{\partial z^2}(z, t) + \frac{s_3^C - r_3^C + 2^3(q_3^C - v_3^C)}{6} \frac{\partial^3 \tilde{x}}{\partial z^3}(z, t) \\
&+ \frac{s_4^C + r_4^C + 2^4(q_4^C + v_4^C)}{24} \frac{\partial^4 \tilde{x}}{\partial z^4}(z, t)
\end{aligned} \tag{49}$$

Topological equivalence: Since the model is nonlinear, the study of the topological equivalence requires a detailed bifurcation analysis, as shown in Example 2.

Example 5 : Let us consider the linear canonical CNN equation, described by the following two-dimensional templates:

$$T^A = 0 \quad T^C = \begin{bmatrix} T_{1,-1}^C & T_{1,0}^C & T_{1,1}^C \\ T_{0,-1}^C & T_{0,0}^C & T_{0,1}^C \\ T_{-1,-1}^C & T_{-1,0}^C & T_{-1,1}^C \end{bmatrix} \quad (50)$$

For the sake of the simplicity we assume that the space steps in both the z and the w dimension are equal (i.e. $h = h_z = h_w$) and that the template coefficients are second order polynomial of the variable $1/h$

$$T_{nm}^C = T_{nm,0}^C + \frac{T_{nm,1}^C}{h} + \frac{T_{nm,2}^C}{h^2} \quad (-1 \leq n \leq 1, -1 \leq m \leq 1) \quad (51)$$

The corresponding canonical CNN equation is reported below:

$$L(D_t)x_{ij}(t) = \sum_{n=-1}^{n=1} \sum_{m=-1}^{m=1} T_{nm}^C x_{i+n,j+m} \quad (1 \leq i \leq N, 1 \leq j \leq M) \quad (52)$$

Approximation: In order to apply the technique shown in Example 1, the explicit Taylor expansions of the quantities below are needed (where $z_i = h i$ and $w_j = h j$):

$$\begin{aligned} \tilde{x}(z_i \pm h, w_j, t) &= \tilde{x}(z_i, w_j, t) \pm \frac{\partial \tilde{x}}{\partial z}(z_i, w_j, t) h + \frac{\partial^2 \tilde{x}}{\partial z^2}(z_i, w_j, t) \frac{h^2}{2} + \dots \\ \tilde{x}(z_i, w_j \pm h, t) &= \tilde{x}(z_i, w_j, t) \pm \frac{\partial \tilde{x}}{\partial w}(z_i, w_j, t) h + \frac{\partial^2 \tilde{x}}{\partial w^2}(z_i, w_j, t) \frac{h^2}{2} + \dots \\ \tilde{x}(z_i \pm h, w_j \pm h, t) &= \tilde{x}(z_i, w_j, t) \pm \frac{\partial \tilde{x}}{\partial z}(z_i, w_j, t) h \pm \frac{\partial \tilde{x}}{\partial w}(z_i, w_j, t) h \\ &\quad + \frac{\partial^2 \tilde{x}}{\partial z^2}(z_i, w_j, t) \frac{h^2}{2} + \frac{\partial^2 \tilde{x}}{\partial w^2}(z_i, w_j, t) \frac{h^2}{2} + \frac{\partial^2 \tilde{x}}{\partial z \partial w}(z_i, w_j, t) h^2 + \dots \\ \tilde{x}(z_i \pm h, w_j \mp h, t) &= \tilde{x}(z_i, w_j, t) \pm \frac{\partial \tilde{x}}{\partial z}(z_i, w_j, t) h \mp \frac{\partial \tilde{x}}{\partial w}(z_i, w_j, t) h \\ &\quad + \frac{\partial^2 \tilde{x}}{\partial z^2}(z_i, w_j, t) \frac{h^2}{2} + \frac{\partial^2 \tilde{x}}{\partial w^2}(z_i, w_j, t) \frac{h^2}{2} - \frac{\partial^2 \tilde{x}}{\partial z \partial w}(z_i, w_j, t) h^2 + \dots \end{aligned} \quad (53)$$

The quantity $\Gamma_{ij}(t)$ can be computed by using the series expansion above (53). We have:

$$\begin{aligned} \Gamma_{ij}(t) &= \sum_{n=-1}^{n=1} \sum_{m=-1}^{m=1} T_{nm}^C \tilde{x}(z_i + nh, w_j + mh, t) \\ &= \left[\sum_{n=-1}^{n=1} \sum_{m=-1}^{m=1} T_{nm}^C \right] \tilde{x}(z_i, w_j, t) + \left[\sum_{m=-1}^{m=1} (T_{1,m}^C - T_{-1,m}^C) \right] \frac{\partial \tilde{x}}{\partial z}(z_i, w_j, t) h \\ &\quad + \left[\sum_{n=-1}^{n=1} (T_{n,1}^C - T_{n,-1}^C) \right] \frac{\partial \tilde{x}}{\partial w}(z_i, w_j, t) h + \left[\sum_{n \neq 0} \sum_{m=-1}^{m=1} T_{nm}^C \right] \frac{\partial^2 \tilde{x}}{\partial z^2}(z_i, w_j, t) \frac{h^2}{2} \\ &\quad + \left[\sum_{n=-1}^{n=1} \sum_{m \neq 0} T_{nm}^C \right] \frac{\partial^2 \tilde{x}}{\partial w^2}(z_i, w_j, t) \frac{h^2}{2} + (T_{11}^C + T_{-1,-1}^C - T_{1,-1}^C - T_{-1,1}^C) \frac{\partial^2 \tilde{x}}{\partial z \partial w}(z_i, w_j, t) h^2 \\ &\quad + \dots \end{aligned} \quad (54)$$

As in Example 1, it is required the coefficients of the above expression (54) be finite as $h \rightarrow 0$. We have the following constraints:

$$\begin{aligned}
\sum_{n=-1}^{n=1} \sum_{m=-1}^{m=1} T_{nm,1}^C &= 0 & \sum_{n=-1}^{n=1} \sum_{m=-1}^{m=1} T_{nm,2}^C &= 0 \\
\sum_{m=-1}^{m=1} (T_{1,m,2}^C - T_{-1,m,2}^C) &= 0 & \sum_{n=-1}^{n=1} (T_{n,1,2}^C - T_{n,-1,2}^C) &= 0
\end{aligned} \tag{55}$$

By computing the quantity $\Delta_{i,j}$ (see Def. 5) we obtain that, if Eqs. (55) are fulfilled, the canonical CNN equation approximates the following PDE for $h \rightarrow 0$:

$$\begin{aligned}
L(D_t)[\tilde{x}(z, w, t)] &= \left[\sum_{n=-1}^{n=1} \sum_{m=-1}^{m=1} T_{nm,0}^C \right] \tilde{x}(z, w, t) + \left[\sum_{m=-1}^{m=1} (T_{1,m,1}^C - T_{-1,m,1}^C) \right] \frac{\partial \tilde{x}}{\partial z}(z, w, t) \\
&+ \left[\sum_{n=-1}^{n=1} (T_{n,1,1}^C - T_{n,-1,1}^C) \right] \frac{\partial \tilde{x}}{\partial w}(z, w, t) + \frac{1}{2} \left[\sum_{n \neq 0} \sum_{m=-1}^{m=1} T_{nm,2}^C \right] \frac{\partial^2 \tilde{x}}{\partial z^2}(z, w, t) \\
&+ \frac{1}{2} \left[\sum_{n=-1}^{n=1} \sum_{m \neq 0} T_{nm,2}^C \right] \frac{\partial^2 \tilde{x}}{\partial w^2}(z, w, t) \\
&+ \left(T_{11,2}^C + T_{-1,-1,2}^C - T_{1,-1,2}^C - T_{-1,1,2}^C \right) \frac{\partial^2 \tilde{x}}{\partial z \partial w}(z, w, t)
\end{aligned} \tag{56}$$

If Eqs. (55) are not satisfied the canonical CNN equation does not approximate any PDE model and hence does not converge to any PDE.

Topological equivalence: since the model is linear, the considerations of Example 1 hold.

Example 6 : As a final example let us consider the nonlinear canonical CNN equation, described by the following two-dimensional templates:

$$T^A = \begin{bmatrix} T_{1,-1}^A & T_{1,0}^A & T_{1,1}^A \\ T_{0,-1}^A & T_{0,0}^A & T_{0,1}^A \\ T_{-1,-1}^A & T_{-1,0}^A & T_{-1,1}^A \end{bmatrix} \quad T^C = \begin{bmatrix} T_{1,-1}^C & T_{1,0}^C & T_{1,1}^C \\ T_{0,-1}^C & T_{0,0}^C & T_{0,1}^C \\ T_{-1,-1}^C & T_{-1,0}^C & T_{-1,1}^C \end{bmatrix} \tag{57}$$

with

$$T_{nm}^{A,C} = T_{nm,0}^{A,C} + \frac{T_{nm,1}^{A,C}}{h} + \frac{T_{nm,2}^{A,C}}{h^2} \quad (-1 \leq n \leq 1, -1 \leq m \leq 1) \tag{58}$$

The corresponding canonical CNN equation is reported below:

$$L(D_t)x_{ij}(t) = \sum_{n=-1}^{n=1} \sum_{m=-1}^{m=1} T_{nm}^A f(x_{i+n,j+m}) + \sum_{n=-1}^{n=1} \sum_{m=-1}^{m=1} T_{nm}^C x_{i+n,j+m} \quad (1 \leq i \leq N, 1 \leq j \leq M) \tag{59}$$

Approximation: By proceeding as in Example 1, we find that the canonical CNN equation (59) approximates a PDE if and only if the following constraints are fulfilled:

$$\begin{aligned}
\sum_{n=-1}^{n=1} \sum_{m=-1}^{m=1} T_{nm,1}^{A,C} &= 0 & \sum_{n=-1}^{n=1} \sum_{m=-1}^{m=1} T_{nm,2}^{A,C} &= 0 \\
\sum_{m=-1}^{m=1} (T_{1,m,2}^{A,C} - T_{-1,m,2}^{A,C}) &= 0 & \sum_{n=-1}^{n=1} (T_{n,1,2}^{A,C} - T_{n,-1,2}^{A,C}) &= 0
\end{aligned} \tag{60}$$

The corresponding PDE is:

$$\begin{aligned}
L(D_t)[\tilde{x}(z, w, t)] &= \left[\sum_{n=-1}^{n=1} \sum_{m=-1}^{m=1} T_{nm,0}^A \right] f[\tilde{x}(z, w, t)] + \left[\sum_{m=-1}^{m=1} (T_{1,m,1}^A - T_{-1,m,1}^A) \right] \frac{\partial f[\tilde{x}(z, w, t)]}{\partial z} \\
&+ \left[\sum_{n=-1}^{n=1} (T_{n,1,1}^A - T_{n,-1,1}^A) \right] \frac{\partial f[\tilde{x}(z, w, t)]}{\partial w} + \frac{1}{2} \left[\sum_{n \neq 0} \sum_{m=-1}^{m=1} T_{nm,2}^A \right] \frac{\partial^2 f[\tilde{x}(z, w, t)]}{\partial z^2} \\
&+ \frac{1}{2} \left[\sum_{n=-1}^{n=1} \sum_{m \neq 0} T_{nm,2}^A \right] \frac{\partial^2 f[\tilde{x}(z, w, t)]}{\partial w^2} \\
&+ \left(T_{11,2}^A + T_{-1,-1,2}^A - T_{1,-1,2}^A - T_{-1,1,2}^A \right) \frac{\partial^2 f[\tilde{x}(z, w, t)]}{\partial z \partial w} \\
&+ \left[\sum_{n=-1}^{n=1} \sum_{m=-1}^{m=1} T_{nm,0}^C \right] \tilde{x}(z, w, t) + \left[\sum_{m=-1}^{m=1} (T_{1,m,1}^C - T_{-1,m,1}^C) \right] \frac{\partial \tilde{x}}{\partial z}(z, w, t) \\
&+ \left[\sum_{n=-1}^{n=1} (T_{n,1,1}^C - T_{n,-1,1}^C) \right] \frac{\partial \tilde{x}}{\partial w}(z, w, t) + \frac{1}{2} \left[\sum_{n \neq 0} \sum_{m=-1}^{m=1} T_{nm,2}^C \right] \frac{\partial^2 \tilde{x}}{\partial z^2}(z, w, t) \\
&+ \frac{1}{2} \left[\sum_{n=-1}^{n=1} \sum_{m \neq 0} T_{nm,2}^C \right] \frac{\partial^2 \tilde{x}}{\partial w^2}(z, w, t) \\
&+ \left(T_{11,2}^C + T_{-1,-1,2}^C - T_{1,-1,2}^C - T_{-1,1,2}^C \right) \frac{\partial^2 \tilde{x}}{\partial z \partial w}(z, w, t)
\end{aligned} \tag{61}$$

Topological equivalence: The same considerations, developed in Example 2, apply.

5 Conclusion

We have investigated the relationship between canonical CNN equations, which are Cellular Partial Difference-Differential Equations (CPDDEs) and PDEs. We have rigorously defined the notion of equivalence between a canonical CNN equation and a PDE and we have shown that such a concept can be split into two problems: approximation and topological equivalence. We have developed a general technique, based on Taylor series expansion, for verifying that a canonical CNN equation approximates a PDE; then we have shown that the study of the topological equivalence can be carried out through bifurcation analysis, by assuming as bifurcation parameters the space discretization steps.

Finally we have reported some significant examples, that show that there exist canonical CNN equations that are not equivalent to any PDE, either because they do not approximate any PDE model, or because they are not topologically equivalent to the PDE that approximate. This shows that the CNN spatio-temporal dynamics is expected to be broader than PDE dynamics.

References

- Ames, W.F. [1977] *Numerical methods for partial differential equations* (Academic Press, New York - San Francisco).
- Chua, L. O. & Yang, L. [1988a] "Cellular neural networks: Theory," *IEEE, Trans. Circuits Syst.* **35**, 1257-1272.
- Chua, L. O. & Yang, L. [1988b] "Cellular neural networks: Applications," *IEEE, Trans. Circuits Syst.* **35**, 1273-1290.
- Chua, L. O. & Roska, T. [1993a] "The CNN paradigm," *IEEE, Trans. Circuits Syst.-I* **40**, 147-156.
- Chua, L. O. & Roska, T. [1993b] "The CNN universal machine: an analogic array computer," *IEEE, Trans. Circuits Syst.-I* **40**, 163-173.
- Chua, L.O., Hasler, M., Moschytz, G.S. & Neiryneck J. [1995] "Autonomous cellular neural networks: a unified paradigm for pattern formation and active wave propagation," *IEEE, Trans. Circuits Syst.-I* **42**, 559-577.
- Chua, L. O. & Roska, T. [2002] *Cellular Neural Networks and Visual Computing* (Cambridge University Press, U.K.)
- Civalleri, P. P. & Gilli, M. [1995] "Circuit models for linear and nonlinear waves," *IEEE, Trans. Circuits Syst.-I* **42**, 578-582.
- Godunov, S.K. & Ryabenkii, V.S. [1987] *Difference schemes: an introduction to the underlying theory* (Elsevier Science Publishers B.V.)
- Keener, J.P. [1987] "Propagation and its failure in coupled systems of discrete excitable cells," *SIAM Journal on Applied Mathematics* **47**, 556-572.
- Kozek, T., Chua, L. O., Roska, T., Wolf, D., Tetzlaff R., Puffer, F. & Lotz, K. [1995] "Simulating nonlinear waves and partial differential equations via CNN - Part II: typical examples," *IEEE, Trans. Circuits Syst.-I* **42**, 816-820.
- Perez Munuzuri, V. & Perez Villar, V. & Chua, L.O. [1993] "Traveling wave front and its failure in a one-dimensional array of Chua's circuits," *J. Circuits, Syst., Comput.* **3**, 211-215, 1993.
- Roska, T., Chua, L. O., Wolf D., Kozek, T., Tetzlaff, R. & Puffer, F. [1995] "Simulating nonlinear waves and partial differential equations via CNN - Part I: basic techniques," *IEEE, Trans. Circuits Syst.-I* **42**, 807-815.
- Serpico, C., Setti, G., Thiran, P. & Pascarelli, A. [1999] "Local diffusion, global propagation and propagation failure in 1D cellular neural networks," in *Proceedings of the International Symposium on Nonlinear Theory and Applications, NOLTA 1999* (Hawaii, USA), pp. 399-402.
- Vázquez, A. R., Delgado-Restituto, M., Roca, E., Linan, G., Carmona, R., Espejo, S. & Dominguez-Castro, R. [2000] "CMOS Analogue Design Primitives," in *Towards the visual microprocessor - VLSI design and use of Cellular Network Universal Machines* (Ed. by T.Roska and A. Rodriguez-Vazquez, J. Wiley, Chichester.) pp. 87-131.
- Whitham, G. B. [1968] *Linear and nonlinear waves* (J. Wiley, New York).

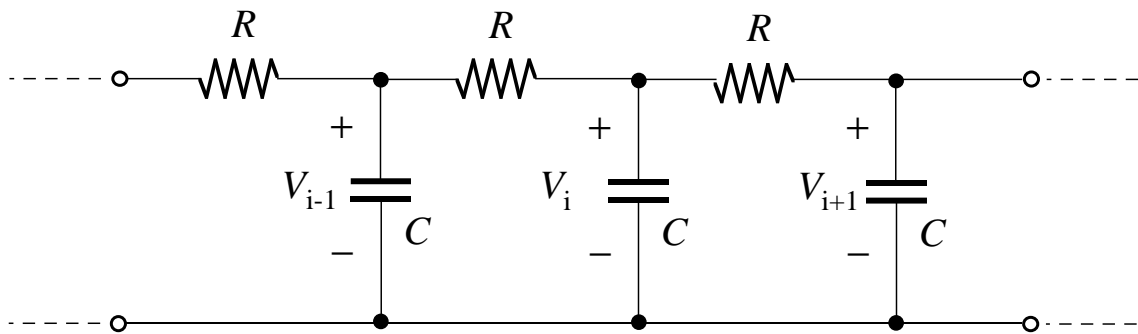


Figure 1: *Chain of lumped RC cells, approximating a RC transmission line.*

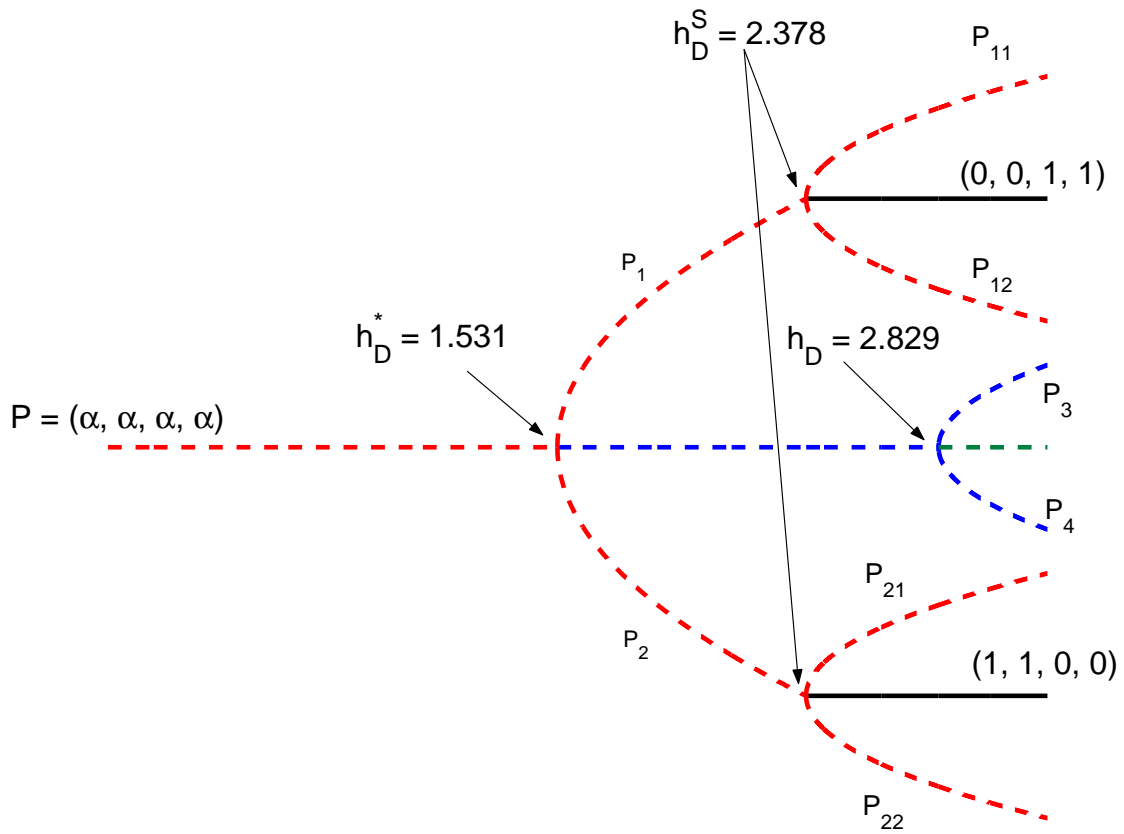


Figure 2: *Equilibrium point bifurcations for the 4 cell canonical CNN equation (37). Saddle points of index 1 are denoted by red lines; saddle points of index 2 are denoted by blue lines; saddle points of index 3 are denoted by green lines; stable nodes are denoted by solid black lines.*

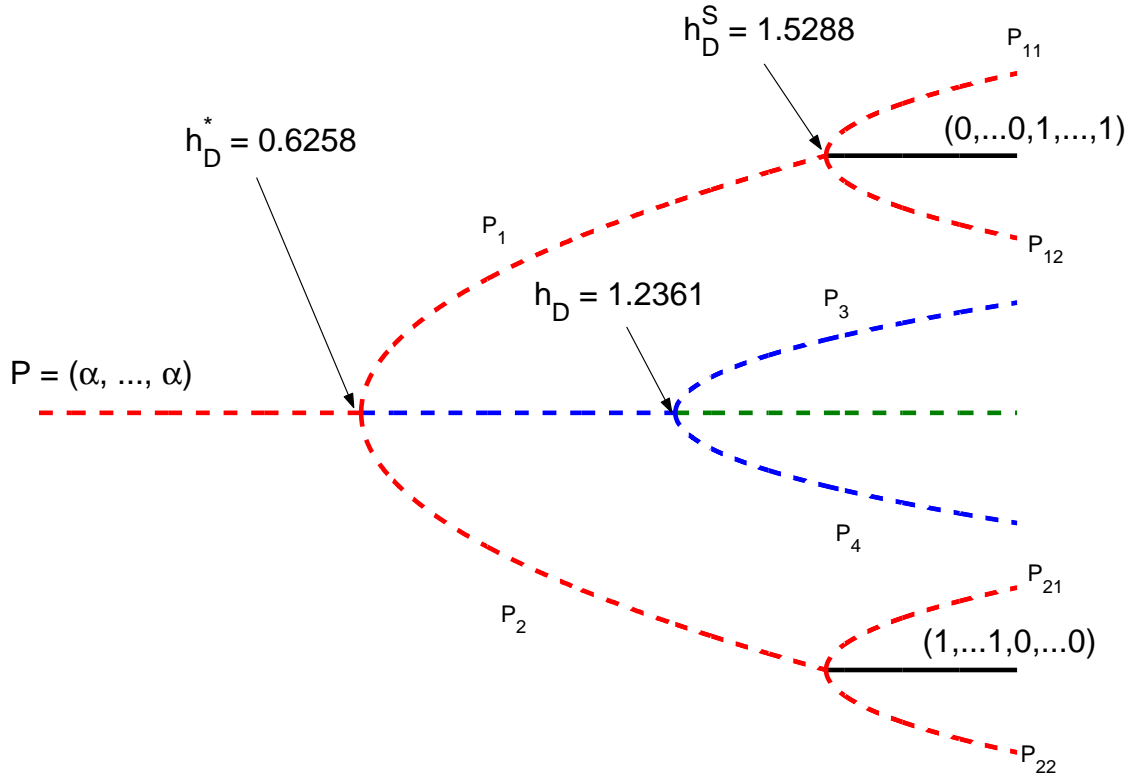


Figure 3: *Equilibrium point bifurcations for the 10 cell canonical CNN equation (37). Saddle points of index 1 are denoted by red lines; saddle points of index 2 are denoted by blue lines; saddle points of index 3 are denoted by green lines; stable nodes are denoted by solid black lines.*

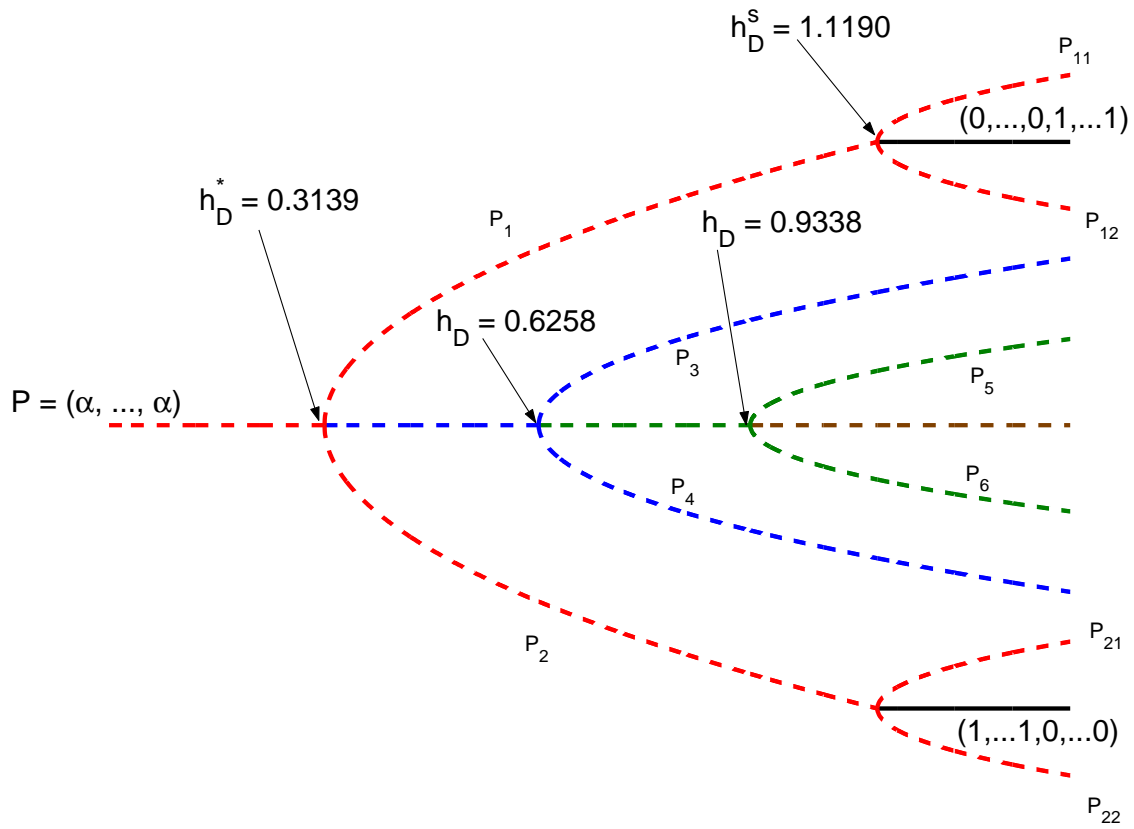


Figure 4: *Equilibrium point bifurcations for the 20 cell canonical CNN equation (37). Saddle points of index 1 are denoted by red lines; saddle points of index 2 are denoted by blue lines; saddle points of index 3 are denoted by green lines; saddle points of index 4 are denoted by brown lines; stable nodes are denoted by solid black lines.*

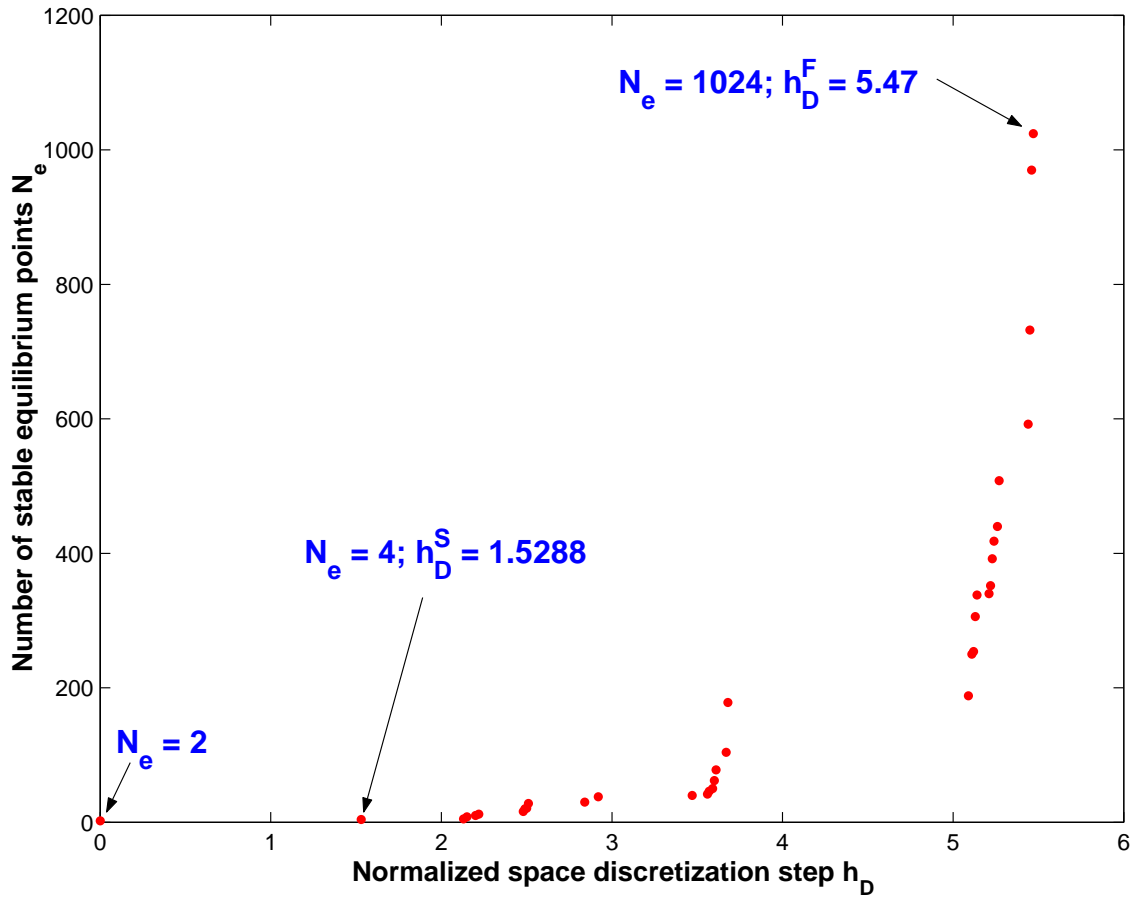


Figure 5: Number of stable equilibrium points N_e versus the normalized discretization step h_D for the 10 cell canonical CNN equation (37).